Human Molecular Genetics, 2004, Vol. 13, No. 19 **2263–2278**
doi:10.1093/hmg/ddh241
Advance Access published on August 18, 2004

Age-associated alteration of gene expression patterns in mouse oocytes

Toshio Hamatani†, Geppino Falco†, Mark G. Carter, Hidenori Akutsu, Carole A. Stagg, Alexei A. Sharov, Dawood B. Dudekula, Vincent VanBuren and Minoru S.H. Ko*

Developmental Genomics and Aging Section, Laboratory of Genetics, National Institute on Aging, National Institutes of Health, 333 Cassell Drive, Suite 3000, Baltimore, MD 21224, USA

Received May 9, 2004; Revised and Accepted July 20, 2004

Decreasing oocyte competence with maternal aging is a major factor in human infertility. To investigate the age-dependent molecular changes in a mouse model, we compared the expression profiles of metaphase II oocytes collected from 5- to 6-week-old mice with those collected from 42- to 45-week-old mice using the NIA 22K 60-mer oligo microarray. Among approximately 11 000 genes whose transcripts were detected in oocytes, about 5% (530) showed statistically significant expression changes, excluding the possibility of global decline in transcript abundance. Consistent with the generally accepted view of aging, the differentially expressed genes included ones involved in mitochondrial function and oxidative stress. However, the expression of other genes involved in chromatin structure, DNA methylation, genome stability and RNA helicases was also altered, suggesting the existence of additional mechanisms for aging. Among the transcripts decreased with aging, we identified and characterized a group of new oocyte-specific genes, members of the human NACHT, leucine-rich repeat and PYD-containing (NALP) gene family. These results have implications for aging research as well as for clinical ooplasmic donation to rejuvenate aging oocytes.

INTRODUCTION

Reproductive capacity in women declines dramatically beyond the mid-30s (1–4). Although the primary cause for this decline is the gradual depletion of oocytes, the decline of oocyte quality is also suggested to play an important role. For example, it has been shown that young women undergoing standard *in vitro* fertilization (IVF) with their own eggs show a success rate comparable with older women (>40 years) undergoing IVF with eggs donated by this younger subset of women (5). Age-related decline in oocyte quality has been associated with aneuploidy because of the age-associated increase of spontaneous abortions and numerical meiotic division errors (6), but the primary cause of such anomalies and other factors determining oocyte quality remains to be elucidated.

The degree to which oocytes age is also relevant to the clinical application of ooplasmic donation (1,7). Ooplasmic donation has been performed by injecting ooplasm from a young healthy donor oocyte into a patient oocyte at metaphase II (MII) stage to improve the outcome of assisted reproduction methods (8,9). Some mouse studies suggested that ooplasmic donation by cytoplasmic injection or by nuclear transfer from an oocyte to another enucleated oocyte has no detrimental effect on development at the MII or germinal vesicle stage (8,10,11) (reviewed in 12), but no direct supporting molecular biological evidence has been reported (13,14). In fact, the premature rupture of membranes and intrauterine fetal death following ooplasmic donation by nuclear transfer from a patient oocyte to an enucleated young donor oocyte (15), and mitochondrial heteroplasmy after birth following ooplasmic injection have been reported very recently (16,17). Thus, studies of molecular mechanisms involved in the decline of oocyte quality with maternal age could have important implications for the efficacy and safety of clinical ooplasmic donation.

Whether oocytes, which are germline-derived and in some sense immortal, age in ways similar to somatic cells is a fundamental question in aging research (18–21). The alteration of gene expression patterns in aging cells and organs has been studied (22,23) and global expression profiling of aging organs has also been performed (24,25). However, oocytes provide unique and challenging material for microarray-based studies of aging.

First, in contrast to organs and continuously cultured fibroblast cells (26), in oocytes all the aging-associated

*To whom correspondence should be addressed. Tel: +1 4105588359; Fax: +1 4105588331; Email: kom@grc.nia.nih.gov
†The authors wish it to be known that, in their opinion, the first two authors should be regarded as joint First Authors.

complications will be imposed on the cell cycle-synchronized and -arrested cells. Most of the primordial follicles are formed during fetal development, though a recent study suggested meiotic entry of germline stem cells in post-natal mammalian ovary (27). Oocytes are arrested and stay in the middle of prometaphase II for more than 40 years in humans and more than a year in mice. At various time points of their adult life, these primordial oocytes with a diameter of 15–20 μm grow to become full-grown oocytes of 70–150 μm (28). The number of mtDNA copies also increases about 100 times (29). Thus, it is reasonable to assume that the microarray analysis will monitor mainly the cumulative results of the transcriptional activity during follicular growth in adult, which takes only a few weeks and the same amount of time for both young and old oocytes.

Second, the analysis of germline aging on a global scale has been hampered by the lack of an expression profiling platform including genes unique to oocytes and by the difficulties of collecting significant numbers of oocytes. With the recent development of a suitable microarray platform (30), we have overcome these problems and have performed expression profiling of oocytes.

RESULTS AND DISCUSSION

Global characteristics of oocyte aging

We collected three sets of 500 MII oocytes from young (5–6 weeks) and those from aged (42–45 weeks) mice—near the end of their reproductive lifespan (Fig. 1A). For brevity, these oocytes are called 'young oocytes' and 'old oocytes' here. As would be the case in a human IVF clinic, only oocytes with good morphology were harvested from superovulated C57BL/6 mice. These oocytes were free of cumulus cell contamination (Materials and Methods). The labeling of these RNAs provided nearly equal amount of fluorescence probes, indicating the initial amount of RNAs was similar. Therefore, a possibility of general decline in transcript abundance can be excluded.

To control sample-to-sample variation, we analyzed three independent sets of pooled oocytes by microarrays. To assess the variations detected by both technical and biological replications, we also carried out two sets of dye-swap experiments. The expression profiling was performed on the NIA 22K 60-mer oligo microarray, which is enriched for genes expressed in stem cells and early embryos, including oocytes (30).

A total of 131 634 experimental data points were generated and analyzed. Using a cut-off for signal intensities (log intensity ≥ 2.3), transcripts of 10 977 genes were scored as present in oocytes (data available at http://lgsun.grc.nia.nih.gov/microarray/data.html). Along with previous reports (31,32), this list provides a repertoire of genes whose transcripts are accumulated through oogenesis and are present in MII oocytes.

Young and old oocytes had very similar gene expression patterns. Only 530 genes (~5%) exhibited statistically significant differences (449 genes for young oocytes and 81 genes for old oocytes) (Fig. 1B and Supplementary Material, Table S1). Furthermore, the fold difference, i.e. log-ratio of these 530 genes, was relatively small (99 genes, > 2-fold; 431 genes, >1.5-fold). Consistent with the identification of bona fide genes, we found that 425 (80.2%) out of the 530 differentially expressed genes were represented as expressed sequence tags (ESTs) in cDNA libraries from unfertilized eggs, fertilized eggs and two-cell embryos (31).

To validate the microarray data further, we also performed real-time quantitative RT–PCR (Q-PCR) analysis in triplicate for 50 selected genes (Figs 1C and D). Poly(A) length, which can be regulated by cytoplasmic polyadenylation element and is involved in mRNA stability in oocyte and early preimplantation embryos, might affect the efficiency of cRNA linear amplification during probe synthesis. To exclude such poly(A) length-dependent bias, we used random hexamer rather than oligo(dT) primers in cDNA synthesis for Q-PCR. Results from the microarrays and Q-PCR were well correlated: the correlation coefficient was 0.80, with a slope of 0.78 (Fig. 1C). The microarrays thus provide reliable gene expression comparisons between young and old oocytes.

Of the 449 genes showing decreased transcript levels with maternal aging, 284 (63.3%) genes were known, whereas 47 (58.0%) of 81 genes showing the increased transcript levels with maternal aging were known. Functional categories of these genes were assigned by Gene Ontology (GO) terms (33), using the MAPPFinder (34,35) (Fig. 2 and Supplementary Material, Fig. S1). We discuss four functional groups.

Genes involved in mitochondrial function, oxidative damages and stress-responses

Most prominent in the list were 'mitochondrial function', 'oxidative damages' and 'stress-responses' (Fig. 2). Genes such as *mt-Nd3*, *mt-Atp6* and *mt-Co1-3*, encoded in the mitochondrial genome and involved in mitochondrial electron transport chain, were more highly expressed in old oocytes. In contrast, genes encoded in the nuclear genome but related to 'energy pathways' and mitochondrial function (such as *Sdha*, known to be an index for mitochondrial activity) were more highly expressed in young oocytes (Fig. 2). These changes suggest a relative decline in ATP production in aging oocytes. In fact, it has been shown that the aging oocytes contain less ATP and have a lower electrical potential at the inner mitochondrial membrane (36). Interestingly, genes categorized in 'nucleotides and ATP metabolism' and 'ATP binding' also showed decreased expression.

A group of genes that provide protection against stress-responses and damages were also downregulated. Notable were oxidative stress/damage-related genes, such as *Sod1* and the thioredoxin family (*Txn1* and *Apacd*) (Fig. 2). *Sod1* is reported to be highly expressed in human oocytes (37) and the addition of *Sod1* protein improves preimplantation development in mouse (38). Thioredoxins are involved in reduction and protection against oxidative stress-induced apoptosis, and the targeted mutation of *Txn1* caused embryonic lethality shortly after implantation (39). Other 'anti-apoptosis' genes, including *Bcl2l10/Diva*, *Nckap1*, *Psip2*, *Ppid*, *Rnf34*, *Bag4* and *Pdcd6ip*, were also downregulated in old oocytes (Fig. 2).

Second, 'chaperones' such as the heat shock 70 kDa proteins (*Hspa4*, *Hspa8* and *Hsp70-4*) and *Cct* genes (*Cct1-3* and *Cct5*), as well as many other genes involved in the

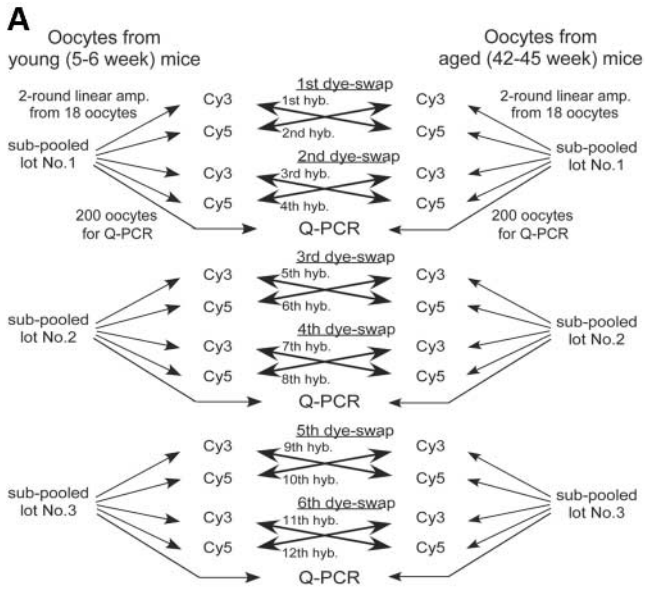

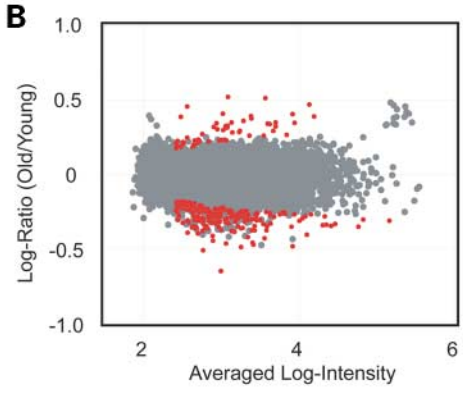

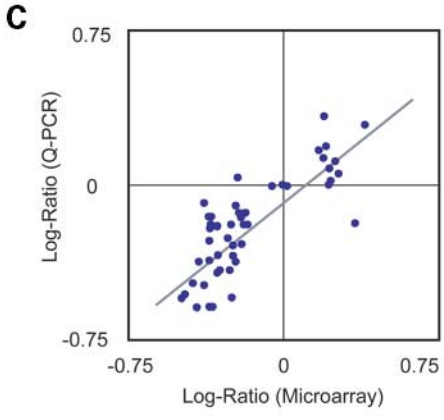

D

Gene	Corresponding NIA clone	Mean of Fold change with aging		Averaged Log-Intensity	P	FDR
		Q-PCR	Microarray			
Gapdh (control gene)	G0119A06	1				
1700023B02Rik/Cir	H3028G12	▲1.54	▲1.620	3.510	0.0046	0.126
Azi2	H3002H06	▼1.23	▼2.392	2.758	5E-10	2E-06
Bmi1	H3114C07	▼2.64	▼1.801	4.507	0.0013	0.067
Bmpr2	L0908G06	▲1.35	▲1.575	2.432	0.0008	0.048
Smc4l1	L0216E11	▼2.64	▼2.013	3.244	0.0034	0.109
Chaf1a	H3087E05	▼3.98	▼2.170	3.088	0.0451	0.409
Camk2g	H3093E05	▲1.08	▼1.648	2.837	0.0042	0.120
Cggbp1	H3084C08	▼1.38	▼1.627	2.705	0.0028	0.098
Crsp6	H3031G01	▼4.02	▼2.585	2.890	7E-07	5E-04
Csnk1e	J0243D09	▲1.30	▲1.798	4.272	0.0014	0.070
Ddx4/Vasa	H3134G04	▼1.57	▼1.547	2.751	0.0018	0.078
Dmap1	H3105G05	▼2.71	▼2.074	3.111	0.0238	0.304
Dnmt1o	G0112B12	▼1.61	▼2.069	3.304	0.0002	0.020
Dnmt1s	G0112B12	▼6.02	▼2.069	3.304	0.0002	0.020
Dnmt3a	H3086G02	▼1.02	▼1.124	2.497	0.3371	0.743
Dnmt3b	H3003C03	▲2.17	▲1.589	3.601	0.0066	0.150
Dnmt3L	NP	▼2.39	NP			
Ezh2	L0244F07	▼2.40	▼1.689	4.341	0.0042	0.120
Fxr2h	L0303E12	▼1.84	▼1.844	3.115	0.0449	0.408
Hdac2	H3123B05	▼1.27	▼1.683	2.992	0.0006	0.042
Hmgb3/Hmg4/Hmg2a	G0117C11	▼2.23	▼2.058	2.852	0.0006	0.041
Kpna2/Importin alpha	H3043A09	▼4.00	▼2.252	2.682	6E-05	0.010
Topors/p53bp3	C0198A05	▼2.36	▼2.260	2.625	6E-10	2E-06
4921520L01Rik /Nalp iota	J0421F06	▼3.46	▼2.951	3.417	7E-05	0.011
2810429C13Rik: similar to TOPBP1 [Homo sapiens]	K0635G09	▼3.61	▼1.765	2.856	0.0006	0.042
Mater	H3102E07	▼2.39	▼2.538	4.103	0.0004	0.032
Morf4l2/Mrgx	C0205C12	▼1.44	▼2.276	3.279	6E-07	5E-04
Msh3	C0259G01	▼1.45	▼1.593	3.077	0.0025	0.094
Nek2	H3035F11	▼1.39	▼1.613	2.737	0.0006	0.041
Nfkbia/ IκBα	H3026A08	▲1.96	▲2.493	3.385	4E-08	7E-05
Nin	H3095C12	▼1.64	▼2.240	2.968	0.0006	0.042
Oosp1	H3085D09	▲1.13	▲1.862	3.843	0.0004	0.031
Paip2	H3105H03	▼3.62	▼3.069	3.259	1E-05	0.004
Pms1	C0216A04	▼2.24	▼1.738	2.704	4E-05	0.007
Ptbp1	H3010A04	▼1.55	▲2.245	3.138	3E-07	3E-04
Rbbp4	J0820F10	▲1.47	▲1.501	3.644	0.0168	0.256
Sin3a	K0515H06	▲1.04	▲1.702	4.041	0.0031	0.104
Madh1	C0218D02	1.00	▲1.668	3.443	0.0023	0.090
Smarca2/Brm	L0215E07	▼1.38	▼1.505	3.194	0.0405	0.384
Sod1	H3130B11	▼1.99	▼1.736	3.647	0.0675	0.476
Tcp1	C0203D04	▼6.25	▼1.549	2.970	0.0092	0.188
Tert	gi3005591	▼1.96	▼1.577	2.705	0.0010	0.056
Tgfb1i4	L0004F04	▲1.20	▲1.688	4.145	0.0039	0.116
Trim24/Tif1a	C0845D01	▼1.90	▼2.258	2.958	0.0014	0.070
Wrnip	H3096C01	▼1.39	▼1.536	3.143	0.0070	0.162
Zfp68	J0248E06	▼1.58	▼2.220	3.219	5E-05	0.008
Zp1	gi6677652	▼1.60	▼2.072	2.986	0.0002	0.025
Zp2	L0236H05	▼3.12	▼2.387	3.362	0.0083	0.178
Zp3	J0918G04	▼3.06	▼2.707	3.922	0.0040	0.118

Figure 1. Microarray gene expression profiles from oocytes of old (old oocytes) and young (young oocytes) mice. (**A**) RNAs were extracted from three sub-pooled lots of approximately 500 oocytes at each age, and samples corresponding to 18 oocytes were separately labeled by two rounds of linear amplification, then hybridized to arrays in duplicate dye-swap pairs. The microarray results for selected genes in the same RNA preparations were validated by quantitative real-time RT–PCR (Q-PCR) in triplicate. (**B**) A scatter plot of all 21 393 features on NIA 22K 60-mer oligo microarray, comparing gene expression of young and aged oocytes. Microarray data for 21 939 probes were analyzed by ANOVA-FDR statistics (30). The combined results of 12 hybridizations identified 530 differentially expressed genes (red circles). (**C**) Comparison of log-ratio results from microarray with those from Q-PCR. Using the same RNA preparations 50 selected genes were validated by Q-PCR in triplicate. The correlation coefficient was 0.80 and the slope was 0.78. (**D**) The fold changes between old and young oocytes by the microarray and Q-PCR analysis about the 50 genes.

A

	Category	Differentially-expressed genes in unfertilized eggs from young mice
1	Mitotic cell cycle and Regulation of cell cycle	*Ccna2, Ccnb2, Cdc16, Cdc2a, Cdc7l1, Nek1, Nek2, Bub1, Mcmd6, Tfdp2, Pold3, Cul1, Spin, Prim2, Tert, Msh3, Ube1c, Hcapg, Ptma, Nin, Smc4l1, Ndn, Sugt1, Vcp, Topors, Mdm4, Carf, Anapc4, Crk, Kras2, Pik3cb, Pank2, Kpna2*
	M phase	*Ccna2, Ccnb2, Cdc16, Cdc2a, Cdc7l1, Nek1, Nek2, Bub1, Ptma, Tfdp2*
	DNA replication	*Mcmd6, Prim2, Msh3, Pold3, Rfc3, Eif2ak4, 2810429C13Rik/Topbp1, Hcapg*
	Genome stability	*Gtf2h1, Pms1, Exo1, Msh3, Tert, Cggbp1, Smc4l1, Nin, Dbd2, Hcapg, 2810429C13Rik/Topbp1, Ube1a, C868987/Ung2, Ddb2*
	Chromosome segregation	*Smc4l1, Nin, Pcnt2*
2	Microtubule cytoskelton	*Hook1, Tuba2, Tubd1, Dncic2, Kif3b, Rnf19/Dorfin , Pcnt2, Nin, Znf212*
3	Chaperone Response to stress	*Cct2, Cct3, Cct5, Tra1, Dnaja1, Dnajb6, Hsp86-1, Hspa4, Hsp70-4, Hspa8, Vbp1* *Tra1, Dnaja1, Hsp86-1, Hspa4, Hspa8, Mmp2, Stk25, Map4k5, Ndr4*
4	Ubiquitine-proteasome pathway	*Hip2, Ubc, Ube1c, Ube2a, Ube2e3, Ube2g1, Usp1, Usp30, 4833420O05Rik/Usp38, Pama6, Pamb1, Psmb4, Psmc2, Psmc3, Psmd12, Siah2, Sugt1, Ga17, Anapc4, D11Moh35, Rnf19/Dorphin, 2700084L22Rik, 6330590F17Rik*
5	Translation factor	*Eef1a1, Eif2ak4, Eif3s6ip, Eif2b3, Eif2b4, Eif3s4, Eif4e, Tcea3, 2010004J23Rik/Rpl4, Wbscr1, Hbs1, 2600017A12Rik/Htatsf1, 1500010B24Rik/Eifay*
6	Nucleotide and ATP metabolism	*Atp2c1, Atp5a1, Atp5b, Atp6v1d, Atp6v1c1, Atp10a, Tyms, Adss2, Mtap, Gmps*
7	Reproduction including Gamatogenesis	*Spin, Kit, Tubd1, Hook1, Zipro1, Zp1, Zp3, Rnf4, Hsf2bp, Mater, Ddx4/Vasa, Arl4, Ssfa2, Padi5/ePAD, Golga3, Fem1a, Rnf19/Dorfin*
	Oocyte-specifi genes including unknown genes (based on EST frequency)	*Zp1, Spin, Ddx4/Vasa, Mater, LOC233001/Nalp9a/Nalp theta, 4921520L01Rik/Nalp iota, E330024M09/Nalp gamma, U020692, Rnf35/2czf61, C330039G02Rik, E330034G19Rik, Etohd4/Fgd6, Bcl2l10/Diva, Padi5/ePAD, LOC381703/AW538212, BC052883, Rdx, Sfmbt, 3230401D17Rik, U048727/U090157, E330017N17, 1810015H18Rik*
8	Glucose metabolism	*Bpgm, Gapd, Sucla2, Onecut1, Pdhb*
	Energy pathways and Mitochondrial functions	*Bpgm, Gyg1, Gapd, Mod1, Sucla2, Sdha, Arht1, Atp5a1, Vdac3, Abcb6, Noc4, Idh3a, Mrpl9, Mrpl12, Akr1a4, Abcf3, Sucla2, Immt, Cox7a2l, Hmgcl, Opa1, Mrpl12, Cyb5, Atp5b , Timm10, Ndufs3, Pdhb, Sdha, Mftc, Tk2, Supv3l1, Hadhb, Bcl2l10/Diva, 3110004O18Rik/Pmpcb, A330108F03Rik, Mtus1*
9	Regulation of transcription	*Rybp, Rbbp7, Zfp278, Plrg1,Trim24/Tif1a, Ezh2, Tmpo, Crsp6, Azi2, Zfp68/Kraz2, Rnf35/2czf61, Lyar, Phtf, Carhsp1, Bmi1, Onecut1, Zfp216, Zfp212, Zfp91, Sfmbt, Lhx8, AW538212, 1110054H05Rik, Klf4, Gtf2h1, C330039G02Rik, Rdbp, Timeless, Dnmt1, Tcea3, 2600017A12Rik/Htatsf1, LOC218832/Rpc155, MGC47046/Polr2b, E330034G19Rik*
10	Chromosome organization and biogenesis	*Hmgb3, Rybp, Tert, Bmi1, Smc4l1, Shprh, Morf4l2/Mrgx, Rbbp7, AL022779, Hdac2, Myst1, Suv39h1-antisense, Smc4l1*
11	Guanyl nucleotide binding	*Adss2, Arf1, Gnai3, Opa1, Arhh, Eef1a1, Eif2b4, Hbs1l, Kras2, Tuba6, Tubd1, Srp54, Spg3a, Arl4, Arht1, Rhoh, Rab1*
12	ATP-binding	*Atp5a1, Atp5b, F13a, 2310061O04Rik, Abcb6, Abcf3, Atp6v1c1, Atp6v1d, Atp10a, Bub1, Cct3, Ccd5, Cdc2a, Cdc7l1, Nek1, Nek2, Nin, Cdc2a, Mcmd6, Cdc7l1, Bub1, Mdm4, Smc4l1, Vcp, Spg3a, Map2k1/Mek1, Trb2, Rras2, Kras2, Rragc, Arl4, Arf1, Stk25, Map4k5, 2610028F08Rik, Camk2g, Kit, Cct2, Cct3, Cct5, Tra1, Hspa4, Hsp70-4, Hspa8, Hsp86-1, Shprh, Msh3, Gmps, Tk2, Opa1, Supv3l1, Apacd, Rab1, Psmc2, Psmc3, Srp54, Ddx4/Vasa, Dhx32, Dhx36, Ddx46, Ddx48, 2310061O04Rik, 2610528A15Rik, Hbs1l, Eif2ak4, B430108F07Rik, 1300010F03Rik, Mater*
13	Ion transport	*Atp5a1, Atp5b, Vdac3, Atp6v1d, Atp10a, Slc31a2, Slc4a8, Ermelin, Ndfip2*
14	Oxidoreductase	*Cyb5, Scd1, Cyp39a1, Akrla4, Aldh9a1, Fdft1, Cryl1, Xdh, Mod1, Ndufs3, Idh3a, Pdhb, 2010004J23Rik/Rpl4, Cd160, Sdha*
15	Dephosphorylation	*Dusp14, Mtmr7, Ppap2a, Ptpra, Ptprg*
16	Cell siganaling	*Dusp14, Mtmr7, Ppap2a, Ptpra, Ptprg, Igbp1, Eps8, Ssh3bp1, Rras2, Kras2, Rhoh, Rragc, Arl4, Arh, Map2k1/Mek1, Map4k5, Stk25, Crk, Socs3, Trb2, Pik3c3, Pik3cb, Prkar1a, Camk2g, Kit, Shh, Gnai3, Abr Stat4, Arhgef16, Ppfibp2/Liprin 2, Ywhah, Ik, Il7, Arf1, Gpr1, Mkln1, Fnta, Arht1, Inpp5f, Pi4k2a, Ppp2r5e*
17	Post-transcriptional modification	*Ddx4/Vasa, Ddx32, Dhx36, Ddx46, Ddx48, 2310061O04Rik, D1Wsu40e, Raver1, Srp54, Rbm12, Paip2, Upf2 2610528A15Rik, Smu1, Rnaseh1, Sf3b3, Nssr, Papola, Spf30, Grsf1, Pus1, Rnpc2, 2600017A12Rik/Htatsf1*
	RNA helicase	*Ddx4/Vasa, Ddx32, Dhx36, Ddx46, Ddx48, 2310061O04Rik, 2610528A15Rik, Supv3l1*
18	Transferase activity, transferring glycosyl groups	*Fut8, B4galt6, Galnt1, Ggta1, Gyg1*
19	Intracellular protein transport and vesicle trafficking	*Cltb, AI642036, 0610038P07Rik/Ssr3, Chic2, Sec13l, Acbd3/Gocap1, Sec22l2, Stx7, Snap23, Syngr3, Vps26, Gdi3, Copb2, Hrb, Rab1, Vcp, Snx14, Ywhah, Arf1, Hook1*
21	Anti-apoptosis	*Txnl, Apacd, Psip2, Ppid, Rnf34, Tnfaip8, Bag4, Pdcd6ip, Bcl2l10/Diva*
20	Cell communication	*Tm4sf8, Lama2, Plxna2, Pcdhb17, Cdh2, Gja7, Plat, Mmp2, Cd160, Shrm*

B

	Category	Differentially-expressed genes in unfertilized eggs from aged mice
1	TGFbeta receptor signaling pathway	*Madh1, Tgfb1i4, Bmpr2*
2	Protein amino acid phospholylation	*Bmpr2, Ptpn11, Csnk1e, Csnk2a1-rs4, Ppp1r3c, mt-Nd3, Prkce, 4930420O11Rik*
3	Cytoskelton organization and biogenesis	*Krt2-8/EndoA, Myh9, Myo10, Pcm1*
4	M phase of cell cycle Cell cycle	*Sept6, Sin3a* *Pcm1, Pik3r1*
5	Development	*Efnb1, Gli3, Apoe, Tcf12*
6	Mitochondria-encoded genes Mitochondrial function	*mt-Nd3, mt-Co1, mt-Co2, mt-Co3, mt-Atp6* *Aldh4a1, Acaa1*
7	Cell signaling	*Madh1, Bmpr2, Ptpn11, Csnk1e, Prkce, Pik3r1, Btla, Plcg2, 4930420O11Rik, Ppp1r3c, Nfkbia/IκBα*
8	Regulation of transcription	*Madh1, Tgfb1i4, Gli3, BC010250 (SET domain), Dnmt3b, Sin3a, Cir, Wbp11*
9	Apoptosis	*Bcl9, Nupr1, Tnfrsf21, Nfkbia/IκBα*
10	Others	*Clcn2, Rrbp1, Kdelr1, Snrpf, Ptbp1, Rpl37a, Mme, Cpeb3, Ugcg, Midn, Larp, Slc39a10, Senp1*
11	Oocyte-specific genes including unknown genes (based on EST frequency)	*4921522K05Rik, Oosp1, 4933427D06Rik, Nfkbia/IκBα*

Figure 2. Functional characterization of decreased and increased transcripts in oocytes with maternal aging. The most frequent GO terms (33) for differentially expressed genes in young and old oocytes were identified by FDR statistics (FDR $\leq$ 15%) using MAPPFinder (34,35) (Supplementary Material, Fig. S1). Only GO terms that had more than three genes ('number changed in hierarchy' $\geq$ 3) for young oocytes are shown in (**A**). Only GO terms that had more than three genes ('number changed in hierarchy' $\geq$ 2) for old oocytes are shown in (**B**). We further recategorized these frequent GO terms and showed genes that represent each annotation. If NCBI had no gene symbol corresponding to an NIA 60-mer oligo, an U-cluster ID containing the oligo sequence was shown in these panels. 'Oocyte-specific genes' were selected on the basis of the frequencies of corresponding ESTs (31).

'ubiquitin–proteasome pathway', such as *Hip2*, *Ubc*, *Ube1c*, *Ube2a*, *Ube2e3*, *Ube2g1*, *Pama6*, *Pamb1*, *Psmb4*, *Psmc2*, *Psmc3*, *Psmd12*, *Siah2* and *Anapc4*, showed decreased expression in old oocytes (Fig. 2). Oxidative stress during aging is known to be associated with the decline of heat shock response, lysosomal activity and ubiquitin–proteasome pathway in somatic cells (25,40). Age-related deterioration of the capacity to produce active heat shock proteins could lead to the accumulation of damaged proteins, primarily oxidized and glycated proteins (41). The production of ubiquitin is modified during aging, often leading to less free ubiquitin and more ubiquitin–protein conjugates (40). A failure of ubiquitination could contribute to the accumulation of highly damaged proteins, which in turn are effective inhibitors of the proteasome (42).

Third, I kappa B alpha (*Nfkbia*/*IκBα*), which is a suppressor of NF-kappa B, was upregulated. NF-kappa B and I kappa B alpha are found in the mitochondria and have been suggested to regulate expression of mitochondrial genes (43). The suppression of NF-kappa B by I kappa B alpha induced the expression of both cytochrome c oxidase III and cytochrome b mRNA (43). This may explain the up-regulation of I kappa B alpha and cytochrome c oxidases (*mtCo1-3*) in oocytes with maternal aging.

Genes involved in cell cycles, DNA stability and chromosome stability

It is known that cellular ATP deprivation caused by inhibitors of energy metabolism in turn induces a gradual breakdown of actin-containing microfilament bundles (44). Consistent with this notion, transcripts related to 'microtubule cytoskelton' and 'chromosome segregation', including *Hook1*, *Tuba1*, *Tubd1*, *Dncic2*, *Kif3b*, *Rnf19*/*Dorfin*, *Pcnt2*, *Nin* and *Smc4l1*, all decreased with maternal aging (Fig. 2). It has been shown that cytoskeletal alteration could cause the increased frequency of aneuploidy, inhibition of extrusion of the first polar body and increased incidence of cellular fragmentation (reviewed in 45,46). Therefore, the alteration of transcript levels of these genes may be associated with chromosome abnormalities.

Although both young and old oocytes were arrested and synchronized at MII, 'cell cycle' was one of the most conspicuous differences between two cell types (Fig. 2). This suggests that oocytes, normally well equipped for the resumption of the cell cycle after fertilization, lost capacity during maternal aging. Another prominent category was 'genome stability', which includes CGG triplet repeat binding protein-1 (*Cggbp1*), fragile X mental retardation-related protein 2 (*Fxr2h*) and homologs of bacterial MutH/L/S mismatch-repair-related proteins such as *Msh3*, *Exo1* and *Pms1* (Figs 1D and 2). These genes, which are often implicated in accelerated aging syndromes and carcinogenesis in human (47–50), decreased in expressions with maternal aging.

We note that the level of telomerase reverse transcriptase (*Tert*), whose expression decreases during general aging and cellular senescence, decreased with maternal aging (Fig. 2). This is consistent with the notion that short telomeres in the chromosomes of human eggs predict poor prognosis following IVF/embryo transfer (51).

Taken together, these expression changes suggest that old oocytes may be less able to maintain intact chromosomes.

Genes involved in oogenesis, fertilization and preimplantation development

Genes involved in the 'Tgf beta receptor signaling pathway', including *Madh1*/*Smad1* and *Bmpr2*, were upregulated in old oocytes (Fig. 2). It is known that in granulosa cells, *Bmpr2* protein functions as a receptor for *Gdf9* protein, a glycoprotein secreted by the oocyte and capable of stimulating granulosa cell proliferation and inhibiting differentiation (52). Its expression is also observed in some oocytes of primary and early secondary follicles in rat (53). *Smad1* signaling is demonstrated to play a critical function in the initial commitment of the germ cell lineage in mice (54), and its mRNA is recruited to polysomes during oocyte maturation in Xenopus, suggesting a role in oocyte maturation (55). In contrast, genes involved in 'intracellular protein transport and vesicle trafficking', were downregulated in old oocytes (Fig. 2), suggesting the dysregulation of oocyte maturation. Indeed, it has been shown that the presence of brefeldin A, a drug that inhibits protein secretion by blocking membrane trafficking from endoplasmic reticulum to Golgi apparatus (56), blocks oocyte maturation before the assembly of the metaphase I spindle maturation (57). Also, *Stx7* and *Snap23* were downregulated in old oocytes. Their encoded proteins are a part of an integral membrane protein complex termed SNAREs (soluble NSF attachment protein receptors), suggested to be involved in vesicular trafficking and exocytosis of cortical granules derived from the Golgi apparatus in mouse oocytes (58).

A number of genes involved in 'reproduction' and 'oocyte-specific genes' also decreased their expression with aging (Fig. 2). For example, *Vasa*, a DEAD helicase expressed specifically in germ cell lineage and development, along with other 'RNA helicases' including *Ddx32*, *Dhx36*, *Ddx46*, *Ddx48* and *Supv3l1*, were downregulated. Similarly, *Rnf35* and *ePAD*, implicated in cytoskeletal organization in eggs, were also downregulated. Furthermore, all three zona pellucida glycoprotein genes, *Zp1*, *Zp2* and *Zp3*, which play important roles in oogenesis (59), fertilization and subsequent preimplantation development (60–62), were downregulated (Figs 1D and 2). Similarly, genes involved in gametogenesis, such as *Kit*, NIMA (never in mitosis gene a)-related expressed kinase 2 (*Nek2*) and *Zfp38*, were downregulated (Fig. 2).

Genes involved in transcriptional regulation

Decreased expression of many transcription factors was observed in oocytes during maternal aging (Fig. 2). This category includes many zinc finger proteins (*Zfps*), whose zinc-coordinated cysteines are susceptible to attack by reactive oxygen species (ROS), and whose DNA binding activity can be attenuated with age (63,64), and polycomb group genes such as *Bmi1*, *Ezh2*, *Sfmbt1* and *Rybp1*. Polycomb group proteins have been known to play crucial roles in cell fate determination via the assembly of specialized forms of repressive chromatin. Because transcription is globally reduced in mature oocytes and dramatic chromatin remodeling occurs

in fertilized eggs, polycomb group genes may be involved in the control of global transcription in oocytes through nucleosome modification, chromatin remodeling and interaction with general transcription factors. Indeed, the expression of *Bmi1* and *Ezh2*, a polycomb-group transcription repressor, was downregulated. Interestingly, Bmi1 is essential for the self-renewal of adult murine hematopoietic stem cells and neuronal stem cells partly via repression of genes involved in cellular senescence and cell death (65). A null mutation in *Ezh2* (which is upregulated upon fertilization and kept highly expressed during the mouse preimplantation stages) results in early embryonic lethality (66).

Transcripts for both oocyte-specific and somatic forms of maintenance DNA methyltransferase (*Dnmt1o* and *Dnmt1s*, respectively), Dnmt-associated protein-1 (*Dmap1*) and *Dnmt3L*, were also downregulated in old oocytes (Figs 1D, 2 and 3), whereas the level of *de novo* methyltransferase *Dnmt3b* transcript was upregulated (Figs 1D and 2). These specific expression patterns were also observed in WI-38 cultured fibroblast cells undergoing cellular senescence (67), suggesting that oocytes and somatic cells may share common features in aging.

Some genes related to 'chromatin organization and biogenesis' were downregulated in old oocytes (Fig. 2). For example, the expression of histone deacetylase 2 (*Hdac2*), which interacts with *Dnmt1* to represses transcription, was also downregulated, as were histone acetyltransferases, *Myst1* and *Mrgx*, which are related to *Morf*, involved in cellular senescence (68). Changes in these and other chromatin remodeling factors, combined with the specific changes in DNA methyltransferase expression, suggest that chromatin structure and epigenetic mechanisms may be appreciably dysregulated as oocytes age.

Examples of unknown genes: the mouse *Nalp* gene family

Among the unknown genes downregulated with maternal aging, we found several genes homologous to the mouse maternal effect gene (*Mater*) that was also downregulated during aging. *Mater* expression is detected in the cytoplasm of growing oocytes and remains present through the late blastocyst stage (69). It has been shown that *Mater* is essential for the preimplantation development, because the development of $Mater^{-/-}$ embryos is arrested at two-cell stage (69). A human homolog of mouse *Mater* has also been identified (70) and categorized as NACHT, leucine-rich repeat and PYD containing 5 (*NALP5*) (71) on the basis of their protein domain structure. Three unknown genes that showed decreased expression in oocytes during maternal aging were found to fall in the Nalp family (row 7 in Fig. 2A). Their chromosomal loci have been represented by LOC233001, 4921520L01Rik and E330024M09/AU022726 in National Center for Biotechnology Information (NCBI) LocusLink, respectively. Searching for similar genes in the NIA Mouse Gene Index (31), we identified at least five more genes whose ESTs were exclusively from cDNA libraries of unfertilized eggs, fertilized eggs (one-cell embryos) and two-cell embryos as well as Mater. These genes were named *Nalp alpha–Nalp kappa* after the human *NALP* gene family (GenBank accession numbers: *Nalp alpha*, AY596194; *Nalp beta*, AY596195; *Nalp gamma*, AY596198; *Nalp delta*, AY596196; *Nalp epsilon*, AY596197; *Nalp zeta*, AY596203; *Nalp eta*, AY596200; *Nalp theta*, AY596202; *Nalp iota*, AY596199; *Nalp kappa*, AY596201). Interestingly, *Nalp alpha–theta* and *Mater* are clustered on Chromosome 7A. *Nalp iota* is located on Chromosome 7F and *Nalp kappa* is located on Chromosome 13. The complete cDNA sequences of *Nalp gamma–kappa* were obtained by fully sequencing either existing NIA cDNA clones (31) or cDNAs amplified by RT–PCR. The open reading frames (ORFs) of these genes were searched against the Pfam HMM database (72). Except for *Nalp iota* that lacks a PYD domain, all the genes of the mouse NALP family contain NACHT, PYD and leucine-rich repeat domains like the human NALP family genes (Fig. 4A).

The sequences of these genes were very similar to each other and it was thus difficult to assign unambiguously orthologous relationships to human NALP genes. To help to clarify the relationships, we also identified rat genes by searching the human and mouse gene sequences against Ensembl Rat genome sequences by WU-BLAST (73) with additional guidance by synteny and 1st exon search tool (74). Amino acid sequence similarities were analyzed among all the genes in human, mouse and rat, and a phylogenetic tree and dot plots were produced based on a sequence distance method and the Neighbor Joining (NJ) algorithm (Fig. 4B and Supplementary Material, Fig. S2) (75). Searches for the conserved regions of the genomic sequences by PipMaker (http://bio.cse.psu.edu) (76) found no significant similarity in the genomic sequences, other than exons (data not shown). All human gene loci were identified to correspond to the mouse *Nalp alpha* locus on mouse chromosome 7A1 (Fig. 4C). Genes on mouse Chromosome 13 found no corresponding human genomic regions, though the surrounding genes showed clear correspondence to human syntenic regions.

Northern blot analyses with ~300 bp gene-specific probes showed that all genes were specifically expressed in oocytes, with additional testis expression for *Nalp iota* (Fig. 5A). *In situ* hybridization with four representative genes revealed oocyte-specific expression in young ovary (Fig. 6). The genes were expressed in primary oocytes at various follicular stages. Furthermore, the microarray expression profiling during mouse preimplantation stages showed that all the genes are expressed in oocytes but are immediately downregulated after fertilization (32) (Fig. 5B). Mouse NALP family genes are thus rather exclusively expressed in oocytes at all follicle stages, with a presumed role in oogenesis and preimplantation embryos.

We used the RNA interference approach as a first step to analyze a function of mouse NALP gene families. The approach has been successfully used to inhibit the function of specific genes in mouse oocytes (77–80). We decided to use the proven method of injecting plasmid vectors expressing siRNA under the mouse U6 promoter into fertilized eggs (81). We first optimized the condition by injecting various concentration of the control vector into the cytoplasm of fertilized eggs and found that the injection of 1–2 pl of 100 ng/μl vector could achieve the maximum GFP expression without

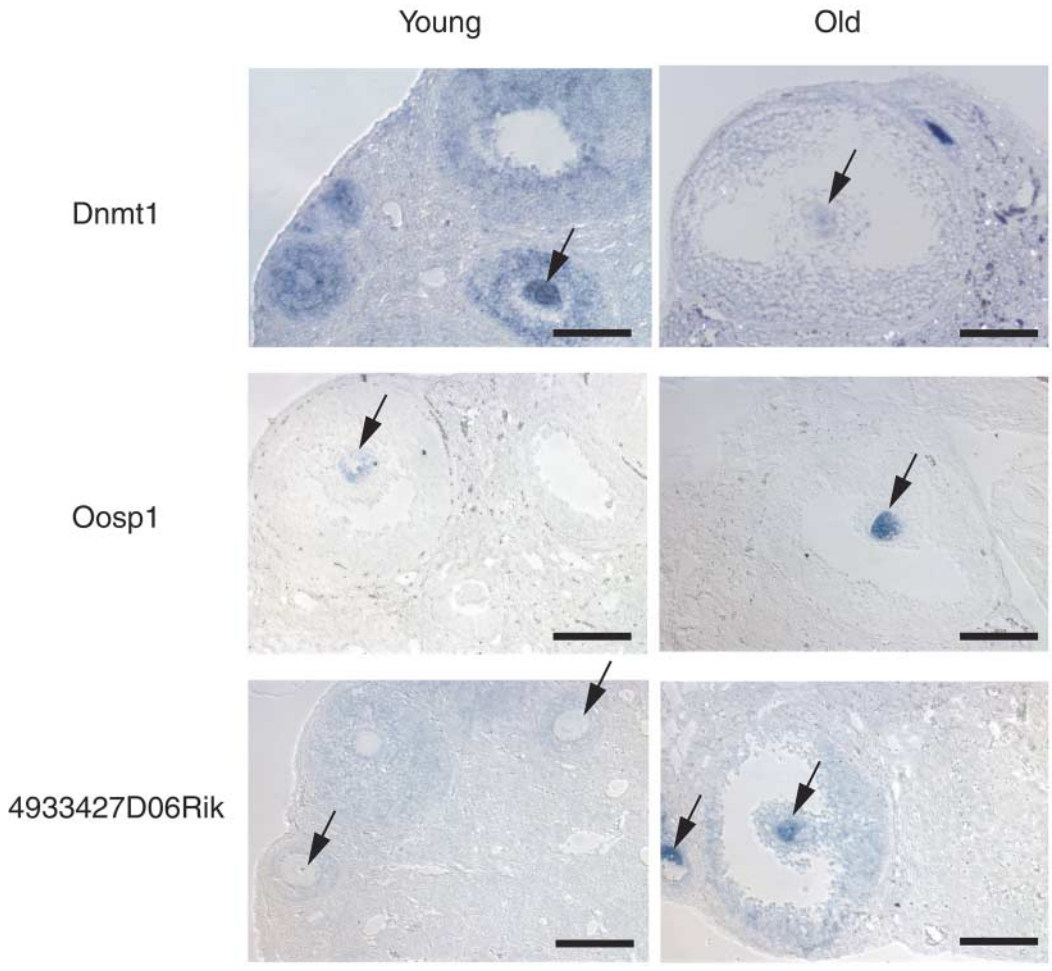

Figure 3. *In situ* hybridization in ovary sections to show the differential gene expression between young and old oocytes. *In situ* hybridization confirmed the microarray results for *Dnmt1*, *Oosp1* and *4933427D06Rik* (bars, 100 μm; arrowheads, oocytes). cDNA inserts from enzyme-digested plasmid DNAs of clone K0853B08, H3085D09 and H3065H07 for *Dnmt1*, *Oosp1* and *4933427D06Rik* were purified and transcribed into digoxigenin-labeled antisense probes, respectively. The *Dnmt1* probe detects both *Dnmt1o* and *Dnmt1s*.

causing the developmental arrest (data not shown). We then carried out three independent experiments by injecting siRNA vector against mouse *Nalp iota* gene into the cytoplasm of mouse fertilized eggs (Materials and Methods). The 80–90% fertilized eggs injected with a control vector expressing a randomized 21-mer sequence developed to blastocysts, whereas only 27–76% of fertilized eggs injected with a vector expressing either siRNA-1 or siRNA-2 developed to blastocyst (Tables 1–3). Although there were some variations, the arrest of development occurred between one-cell and eight-cell stages in most cases. Similar studies targeting a few other unrelated genes did not show any obvious developmental arrest (data not shown). These data suggest that the expression of *Nalp iota* gene is required for the normal development of mouse preimplantation embryos. Because the null mutant mouse of the founding member of this gene family, *Mater/Nalp5*, showed similar developmental arrest (69), the oocyte-specific NALP gene family may play critical role in the preimplantation embryos.

Implications for oxidative stress and oocyte aging

The decline of mitochondrial function fits nicely with the consensus of aging that an increased oxidative damage with time may play an important role in the process of aging. ROS are produced continuously in mitochondria because of leakage of high-energy electrons along the electron transport chain. In contrast to nuclei, mitochondria lack both protective histones and DNA repair activity, and thus can be a primary target of oxidative damage. In fact, the incidence of mtDNA mutations increases in human ovarian tissues after the age of 45 (82). In unfertilized eggs collected from IVF patients, the incidence of mutations in mtDNA increases by 3.3-fold at ages above 38 (83). Morphological abnormalities in oocyte mitochondria from old mice were also observed (84). Thus, it has been suggested that mitochondrial damage by ROS produced over long periods can be a mechanism leading to age-related decline in oocyte quality and chromosomal aneuploidy (45,46,85,86).

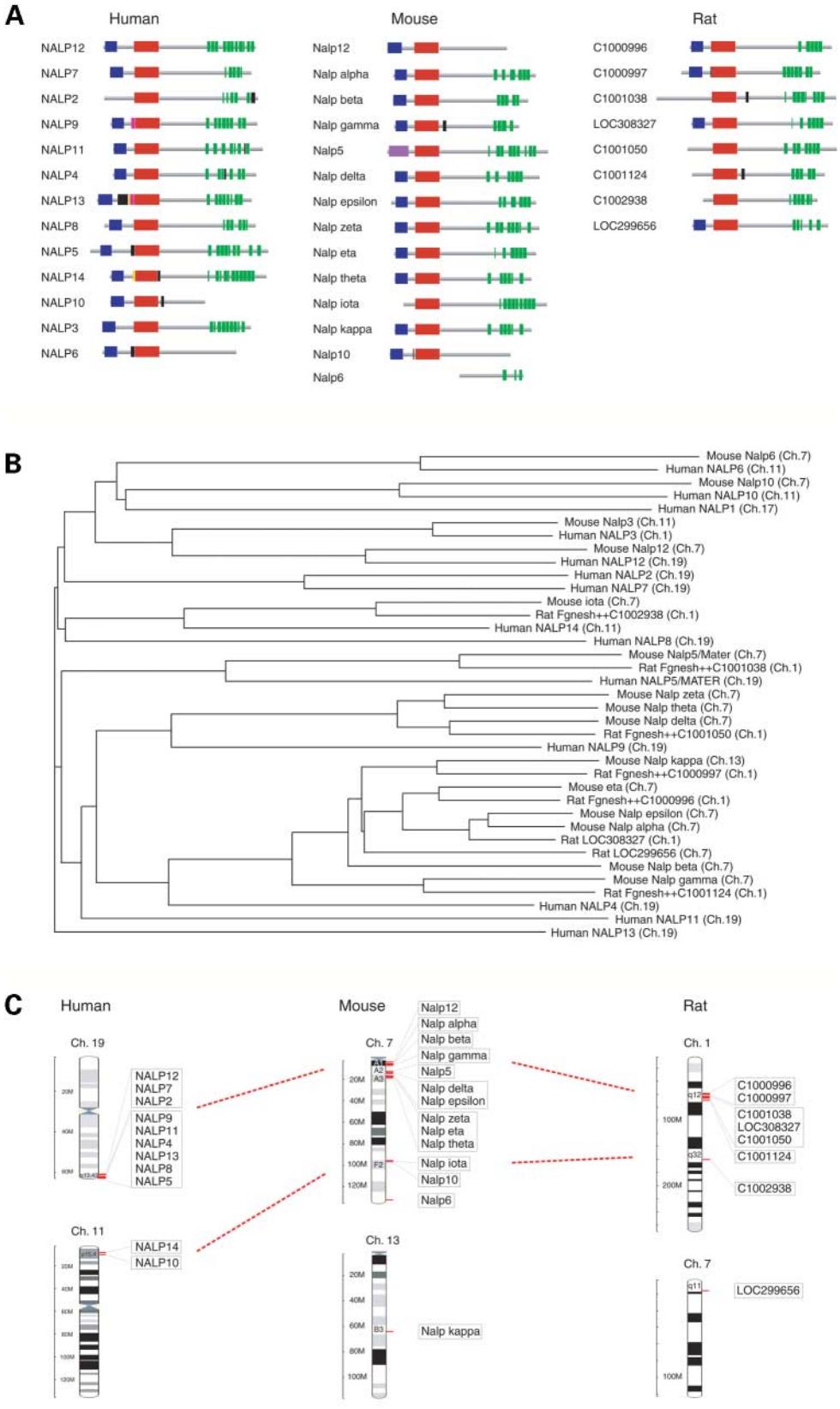

Figure 4. Domains, evolution and chromosomal localization of *Nalp* genes. (**A**) Conserved domains of NALP gene family in human, mouse and rat. PAAD/DAPIN/Pyrin domains, NACHT domains and Leucine-rich repeats are represented by blue, red and green boxes, respectively. (**B**) A dendrogram that shows similarity in amino acid sequences of NALP gene family in human, mouse and rat. (**C**) Chromosomal loci of NALP gene family in human, mouse and rat based on the results of BLAT against UCSC genome assemblies (July 2003, human February 2003, mouse and June 2003; rat).

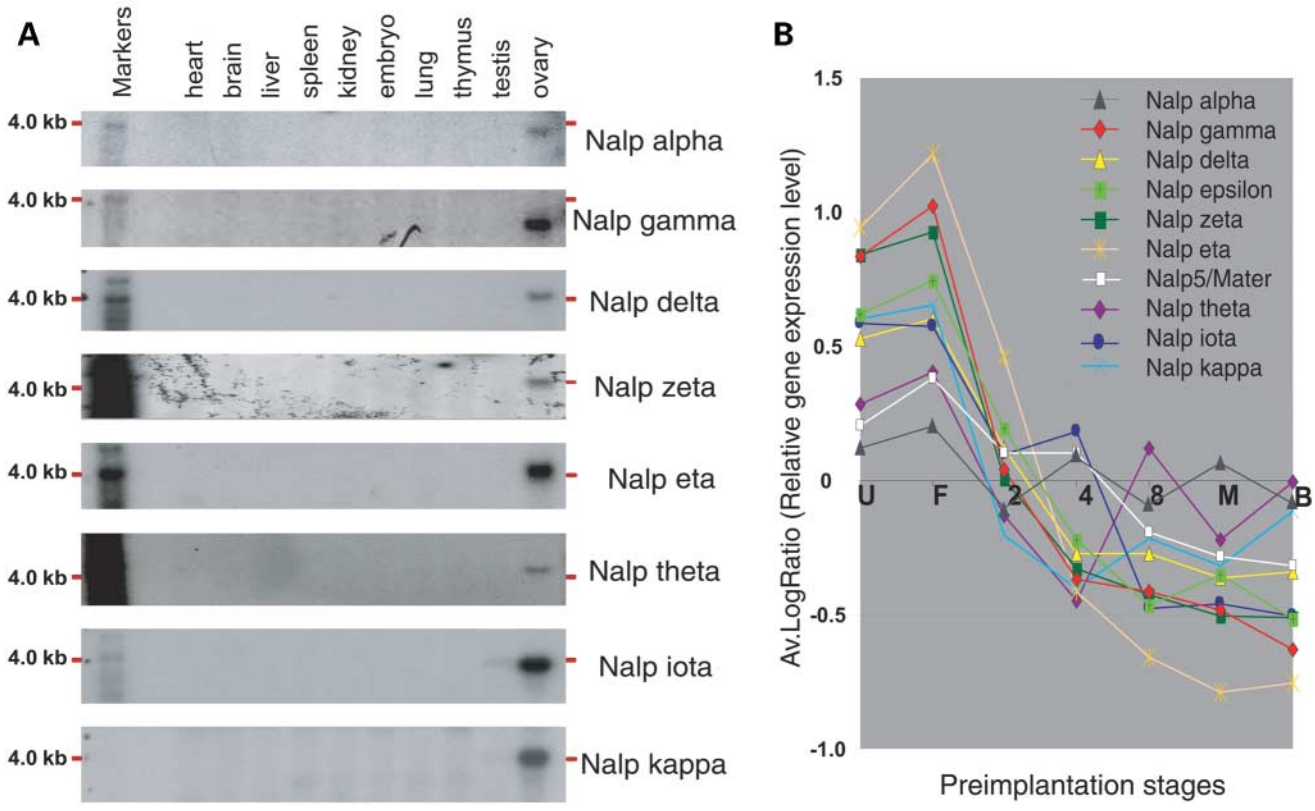

Figure 5. The expression profiles of mouse *Nalp* genes. (**A**) Northern blot analysis using the 300 bp sequences specific to each member of NALP gene family as probes with mouse tissue blot (FirstChoice Mouse Blot 1, Ambion). (**B**) The expression patterns of mouse *Nalp* genes during mouse preimplantation embryo stages based on our previous microarray experiment (32). U, F, 2, 4, 8, M and B denote unfertilized egg, fertilized egg, two-cell embryo, four-cell embryo, eight-cell embryo, morula and blastocyst, respectively.

In this study we also observed an age-related decrease in transcription levels of ATP-related genes that are represented by GO terms such as 'nucleotides and ATP metabolism' and 'ATP binding'. It is known that the depletion of ATP by the decrease of mitochondrial function can decrease the function of proteins that require ATP for their proper function. As such, the microtubule and cytoskeleton proteins seem to be important, because malfunction of these proteins is known to cause failures of chromosome segregation and an accompanying increase of aneuploidy—a major pathological phenotype of old oocytes in humans.

Implications for ooplasmic donation

Discussions about the efficacy and safety of ooplasmic donation have centered on the mitochondria (7). If lowered ATP were the only defect in old oocytes, the injection of ATP could revitalize the oocytes. If the lack of both functional mitochondria and ATP is the problem, ooplasmic donation indeed helps to increase the fertility rate of old oocytes. Our results seem to support this idea, because mitochondria-related genes and ATP-related genes were indeed downregulated in old oocytes. However, our results also suggest that the nucleus of old oocytes may not be competent to produce specific transcripts that are required for normal oocytes, because the microarray analysis primarily revealed the differential RNA levels transcribed from young versus old nuclei during oocyte maturation (Introduction). If the status of the nucleus in old oocytes is already different from that in young oocytes, ooplasmic donation cannot directly correct the problem of old oocytes. Even if nuclei in old oocytes can be reprogramed, such reprograming events are error-prone, as has been demonstrated in mouse and other model systems (87–89).

Implications for germline aging

Although microarray analyses of aging organs and tissues have been reported (24–26), oocyte aging seems to have distinctive features. For example, one of the most conspicuous features of aging in organs such as brain and liver is the inflammatory response, indicated by the upregulation of a number of genes involved in the inflammatory process (24,25). However, such trends were not observed in aging oocytes. One possibility is that these genes are not normally expressed in oocytes, and thus cannot be detected by microarray analysis. Alternatively, the upregulation of inflammatory gene expression in organs merely represents secondary changes during aging, probably due to infiltration of immune cells into organs, but are not seen in single oocytes, especially in the immune privileged environment.

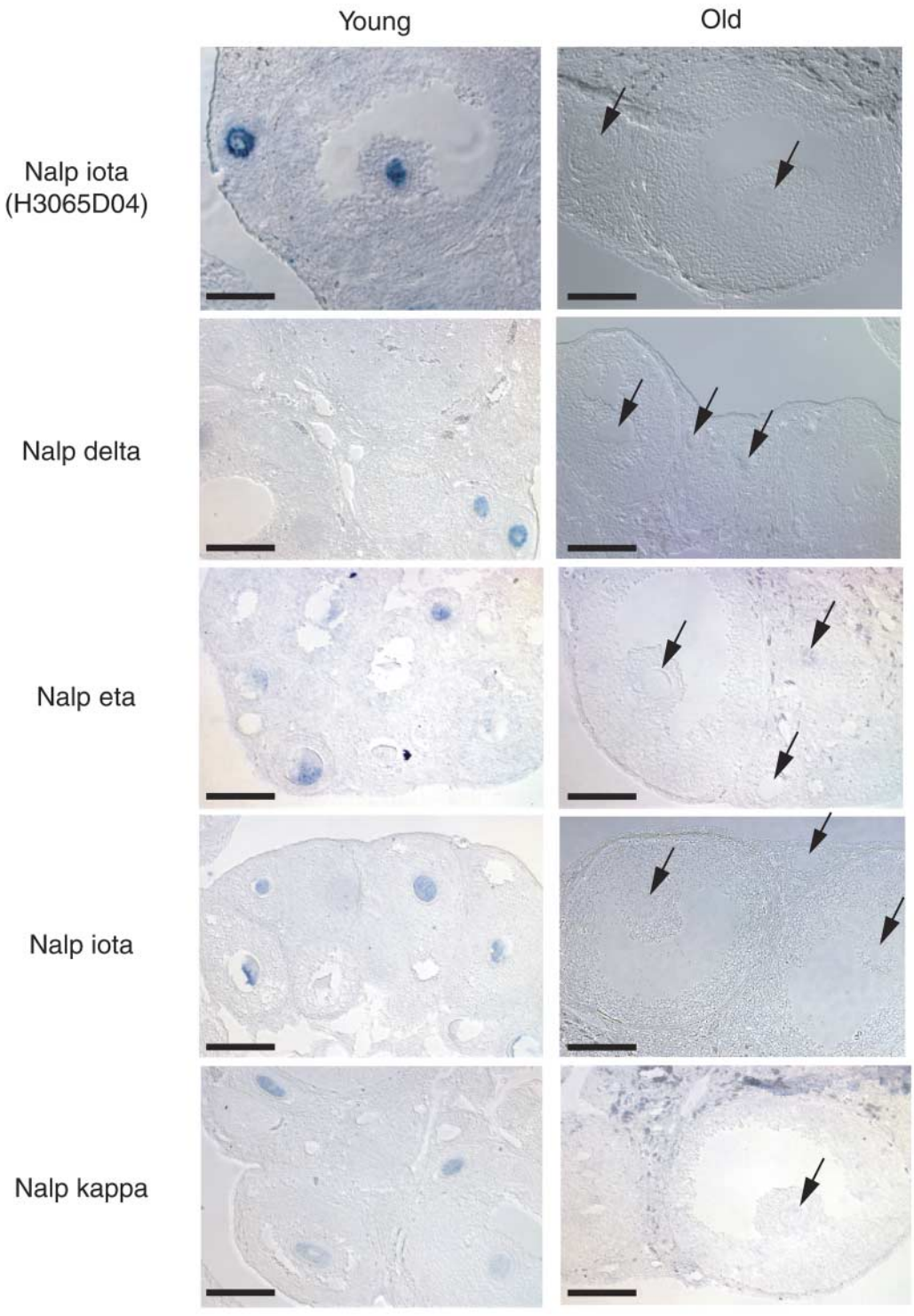

Figure 6. Oocyte expression of *Nalp* genes by *in situ* hybridization. All four *Nalp* genes that we examined showed oocyte-specific expression in young ovary, but faint or no signals in oocytes from aged mice on the same slide (bars, 100 μm; arrowheads in ovary sections from aged mice). The PCR-cloned 300 bp sequences specific to each member of NALP gene family were used as probes.

Another discriminating feature is the insulin-related growth pathway. It is one of the major features of aging at the organism level (90,91). Although the alteration of the 'energy, metabolism pathway' was observed in oocyte aging, genes directly involved in the insulin growth factor pathway were not significantly altered. This may be correlated with the selective use of pyruvate or oxaloacetate rather than glucose as an energy source by oocytes (92,93).

Table 1. Knockdown of *Nalp iota* gene in preimplantation embryos of experiment 1

Vector injected	Number of fertilized eggs injected	Number of embryos arrested at the specific stage			Morula	Blastocyst	Fraction of embryos developed to blastocyst (%)
		One-cell	Two-cell/four-cell	Eight-cell			
Control	33	0	0	3	0	30	90.9
siRNA-1	33	2	11	3	0	17	51.5
siRNA-2	33	0	1	7	0	25	75.8

Table 2. Knockdown of *Nalp iota* gene in preimplantation embryos for experiment 2

Vector injected	Number of fertilized eggs injected	Number of embryos arrested at the specific stage			Eight-cell	Morula	Blastocyst	Fraction of embryos developed to blastocyst (%)
		One-cell	Two-cell	Four-cell				
Control	25	0	1	1	3	0	20	80.0
siRNA-1	34	12	1	2	2	0	17	50.0
siRNA-2	22	4	5	0	7	0	6	27.3

Table 3. Knockdown of *Nalp iota* gene in preimplantation embryos for experiment 3

Vector injected	Number of fertilized eggs injected	Number of embryos arrested at the specific stage			Morula	Blastocyst	Fraction of embryos developed to blastocyst (%)
		One-cell	Two-cell/ three-cell	Four-cell/ eight-cell			
Control	20	0	0	2	0	18	90.0
siRNA-1	19	0	11	2	0	6	31.6
siRNA-2	20	1	5	2	0	12	60.0

Finally, RNA levels of genes involved in the alteration of nuclear status, such as DNA methyltransferases and chromatin remodeling proteins, were clearly different between young and old oocytes, but have not been detected in the previous studies of aging organ or organisms (24,25). It is worth noting that this set of genes overlaps with genes identified for 'stemness', which include genes involved in stress-resistance, chromatin remodeling and DEAD helicase-regulated translation (94). It is thus possible that aging of oocytes is the process where stem cell-like features are being lost from germlines. Indeed, it has been shown that adult stem cells, such as hematopoietic stem cells, tend to lose their self-renewal capacity and differentiation potential during aging (21). This appears to be consistent with recent work that germline stem cells have been found to produce new oocytes in the post-natal mouse ovary (27). However, it remains to be elucidated whether the age-associated gene expression changes observed here are caused by the negative impacts of advancing maternal age on the replicating germline stem cells or cell-cycle arrested oocytes.

MATERIALS AND METHODS

Embryo collection

To model maternal age-related infertility in human patients, we super-ovulated C57BL/6 mice aged 5–6 and 42–45 weeks with injections of 5 IU pregnant mare serum gonadotropin (Sigma, St Louis, MO, USA) and 5 IU human chorionic gonadotropin (hCG) (Sigma) at 65 and 18 h prior to harvest, respectively (Protocol number 220MSK-Mi approved by the NIA Animal Care and Use Committee). The female reproductive lifespan in C57BL/6 mice extends to ~45 weeks, so this time point is a functional approximation of human perimenopause. Oocytes were harvested within a 2 h period, and only those with good morphology were selected, as would be the case in a human IVF clinic. Cumulus cells were removed by incubation in M2 medium (Cell & Molecular Technologies, NJ) with 300 μg/ml hyaluronidase (Sigma), and oocytes were thoroughly washed and transferred to liquid nitrogen for storage. To assess the possible contamination of cumulus cells in these oocyte samples, the expression levels of genes that are well known for their expression in cumulus cells were examined in the microarray data. All three genes examined, *Lhcgr*, *Fshr* and *Star*, showed log-intensitites lower than 2.3, which was used as a cut-off for the presence of the transcripts in this study (Supplementary Material, Table S2). Therefore, it is most unlikely that the microarray data in this report were distorted by the contaminated cumulus cell RNAs.

RNA extraction, labeling and hybridization on the NIA 22K 60-mer oligo microarray

Three subsets of 500 MII oocytes were collected from mice at 5–6 and 42–45 weeks of age, and mRNA was extracted from

each subset using a Quickprep micro poly-A RNA Extraction Kit (Amersham Biosciences, Piscataway, NJ, USA) with linear acrylamide as a carrier (Ambion, Austin, TX, USA). mRNA aliquots equivalent to 36 oocytes from each mRNA subset were labeled with Cy3 and Cy5 dyes by two-round linear amplification labeling reactions to make each cRNA target using a Fluorescent Linear Amplification Kit (Agilent Technologies, Palo Alto, CA, USA) (30). Briefly, mRNA was used to synthesize double-stranded cDNA with moloney murine leukemia virus reverse transcriptase in a reaction scaled down to a total volume of 4 μl, with half the standard T7-oligo-dT primer concentration and 125 ng/μl of T4gp32 single-stranded DNA binding protein (United States Biochemical, Cleveland, OH, USA). Linear amplification (*in vitro* transcription) was performed in a total volume of 16 μl, with half the standard NTP concentration and no labeled CTP. For the second round of amplification, the product of the first reaction was divided in half, and labeled using the manufacturer's standard protocol, with the addition of T4gp32 in the cDNA synthesis reaction. Quality and size distribution of targets were determined by an RNA 6000 Nano Lab-on-chip Assay (Agilent Technologies), and quantitation was determined using a NanoDrop microscale spectrophotometer (NanoDrop, Wilmington, DE, USA). cRNA targets were assembled into hybridizations on the NIA 22K 60-mer oligo microarray (manufactured by Agilent Technologies) (30), forming duplicate dye-swapped pairs for each of three biological replicates (Fig. 1). Compared with a single-round of amplification, the sensitivity of differential expression detection is reduced to 60%, but specificity is retained at 96% using two-round amplification (30).

The microarray contains 21 939 gene features (spots) with 12 223 oligos corresponding to 'genes' defined by having either ORF $\geq$ 100 amino acid. or multiple exons by comparing with the NIA mouse gene index (31). A complete list of annotated gene content of the microarray can be found at the NIA mouse cDNA project web site (http://lgsun.grc.nia.nih.gov/cDNA/cDNA.html).

Microarray data analysis

Intensity values of 21 939 gene features per array were extracted from scanned microarray images using Feature Extraction 5.1.1 software (Agilent Technologies), which performs background subtractions and dye normalization. All primary microarray data and bioinformatic annotations are available at our web site (http://lgsun.grc.nia.nih.gov/microarray/data.html), GEO (http://www.ncbi.nlm.nih.gov/geo/) and ArrayExpress (http://www.ebi.ac.uk/arrayexpress/). Text output was processed using an application developed in-house to perform ANOVA analysis (http://lgsun.grc.nia.nih.gov/ANOVA/). Intensities measured with a $>$ 50% error were replaced with missing values except features with very low intensity. Surrogate values equal to mean error were inserted for values that were negative or less than the probe error. Pair-wise mean comparison was done using *t*-statistics and the false discovery rate (FDR = 15%) method (95). The small number of biological replications typical in expression profiling experiments results in a highly variable error variance, and this problem is usually addressed by log-ratio thresholds (96) that require subjective decisions about biological significance, or by Bayesian adjustment of error variance (97) that may still underestimate error variance and result in false positive results. To reduce false-positives, we opted for a very conservative error model in which the error variance used for estimating *F*-statistics for a feature is the maximum of the actual error variance and the average error variance in 500 features with similar average intensity. Statistical significance was determined using the false discovery rate FDR(=15%) method (95). A scatter plot was created using the NIA microarray analysis tool (http://lgsun.grc.nia.nih.gov/ANOVA/). GenMAPP/MAPPFinder (34,35) were utilized for a functional annotation analysis with GO terms.

Real-time quantitative RT–PCR

The microarray results for selected 50 genes were validated by real-time on an ABI 7700 Sequence Detection System (Applied Biosystems, Foster City, CA, USA) (30). mRNA from each oocyte pool equivalent to 200 oocytes was DNAse-treated (DNA-free, Ambion, Austin, TX, USA), annealed with random hexamer and reverse-transcribed into cDNA with ThermoScript reverse transcriptase (Invitrogen, Carlsbad, CA, USA). Each 15 μl Q-PCR reaction used cDNA equivalent to one-quarter or two oocytes as template. PCR primer pairs were designed using the 3′-sequence of the EST clone such that both primers anneal at 59°C $\pm$ 1°C, the amplicon length is between 105 and 240 bp and low-complexity sequence is avoided (Supplementary Material, Table S3). Primers were tested using ovary cDNA with SYBR Green PCR Master Mix (Applied Biosystems). First, each primer pair was run using a matrix of forward and reverse primer concentrations, and threshold cycle measurements were compared with dissociation curves to determine optimal primer concentrations with high amplicon specificity. Second, a 5-log standard curve dilution series was run using each primer pair at optimal concentration, and amplification efficiencies were calculated. Primer sets with sub-optimal dissociation curves or efficiencies outside of the 85–115% range were discarded, and replacements were designed and tested.

Cloning of the mouse *Nalp* gene family

The NIA Gene Index (http://lgsun.grc.nia.nih.gov/geneindex1/), UCSC Genome Bioinformatics mouse genome assembly (http://genome.ucsc.edu/), Ensemble mouse genome database (http://www.ensembl.org/) and NCBI nucleotide database (http://www.ncbi.nlm.nih.gov/) were blasted with the mouse cDNA sequences of *Mater*, *LOC233001*, *4921520L01Rik* and *E330024M09/AU022726*, and the human NALP cDNA sequences to search for all mouse Mater-like genes. On the basis of predicted full-length transcript sequences for each gene of the Mater-like family, we designed PCR primers to amplify cDNA containing full ORFs for each gene from mouse ovary cDNA. To make mouse ovary cDNA, mouse ovary mRNA was DNAse-treated (DNA-free, Ambion), annealed with oligo-dT primer and reverse-transcribed into cDNA with ThermoScript Reverse Transcriptase (Invitrogen). The PCR-cloned full ORF sequences (Takara Ex Taq

Polymerase, Takara Mirus Bio, Madison, WI, USA; Wizard SV Gel and PCR Clean-Up System, Promega Biosciences, San Luis Obispo, CA, USA; pENTR Directional TOPO Cloning Kit and TOPO XL PCR Cloning Kit, Invitrogen) were sequenced using a BigDye Terminator kit (PE Applied Biosystems, Foster City, CA, USA), DyeEX 96 Kit (Qiagen Valencia, CA, USA) and ABI 3100 Genetic Analyzer (PE Applied Biosystems). To discriminate each gene from other family members in tissue expression analysis, 300 bp sequences unique to each cDNA were selected using Probe Hunter, a software developed in-house (VanBuren *et al.*, manuscript in preparation). We designed primers within these unique 300 bp sequences for each gene (Supplementary Material, Table S4) to amplify the sequences. The PCR-amplified sequences were cloned using a pCR4-TOPO Kit (Invitrogen) and sequenced.

Computational analysis of the mouse Mater-like gene cDNA and human *NALP* gene cDNA sequences

The ORF finder (http://www.ncbi.nlm.nih.gov/gorf/gorf.html) and Pfam HMM databases (http://pfam.wustl.edu/hmmsearch.shtml) were used to analyze the mouse *Nalp* cDNA sequences, identifying ORF and protein domains, respectively. To obtain orthologs and analyze chromosome synteny and nucleotide homology among mouse, rat and human NALPs, Ensemble synteny view (http://www.ensembl.org/Mus_musculus/syntenyview), WU-BALST (http://www.ensembl.org/Multi/blastview) and comparative genomics information in the UCSC genome browser were used. Amino acid sequence similarities were analyzed among all the *NALP* genes in human, rat and mouse, and a phylogenetic tree was postulated on the basis of a sequence distance method and the NJ algorithm of Saitou and Ne (75), using Vector NTI software (Informax, Bethesda, MD, USA).

Northern blot

Northern blot membranes (FirstChoice Mouse Blot 1, Ambion) containing 2 μg of poly(A) RNA per lane isolated from mouse tissues were purchased to detect the expression of Nalps. The 300 bp sequences specific to each member of Nalps were excised from pCR4 vectors and labeled with [α-^{32}P]dCTP as probes. ExpressHyb solution (Clontech) was used for both prehybridization and hybridization. After hybridization at 65°C for 20 h, both membranes were washed twice with 2× SSC at room temperature for 30 min, twice with 2× SSC at 65°C for 30 min and then with 0.1× SSC at 65°C for 30 min, followed by exposure to a PhosphorScreen.

In situ hybridization

In situ hybridization was performed in ovaries from young (6 week) and aged (42 week) C57BL/6 mice. Ovaries were fixed in 4% paraformaldehyde and sectioned (5 μm). Plasmid DNAs were purified from NIA cDNA library clones (H3065D04 for Nalp iota, K0853B08 for Dnmt1s and Dnmt1o, H3085D09 for Oosp1 and H3065D07 for 4933427D06Rik) and pCR4 clones containing Nalp unique 300 bp sequences. The enzyme-digested plasmid DNAs were transcribed into digoxigenin-labeled sense probe controls and antisense probes. The probes were prepared by alkaline hydrolysis and hybridized (60°C, 24 h) to the ovarian sections from young and aged mice, placed on the same slides.

Knockdown of *Nalp iota* gene in preimplantation embryos

Plasmid vectors expressing an siRNA against mouse *Nalp iota* constitutively were constructed by inserting the following 21-mer target sequences (shown in bold) in pRNAT-U6.1/Neo (GeneScript Corp., Scotch Plains, NJ, USA): siRNA-1, GGATCCC**AGCTGCAGATATAGTATGTGA**CTTCCTGT CA**TCACATACTATATCTGCAGCT**TTTTTTCCAAAAG CTT; siRNA-2, GGATCCCG**TTACATCGACCAGAAAC TTCT**CTTCCTGTCA**AGAAGTTTCTGGTCGATGTAA**T TTTTTCCAAAAGCTT, and control (randomized 21-mer), GGATCCC**AGAGACATAGAATCGCACGCA**CTTCCTG TCA**TGCGTGCGATTCTATGTCTCT**TTTTTTCCAAAA GCTT. This vector contains GFP marker under CMV promoter. Fertilized eggs were harvested at 21 h post-hCG from mated superovulated C57BL/6J mice (4–5-week-old) by the standard method (98). After removing cumulus cells by 300 μg/ml hyaluronidase (Sigma) in HEPES-buffered modified Chatot, Ziomek, Bavister (CZB) medium, followed by thorough washing by HEPES-buffered CZB medium, fertilized eggs with good morphology were selected. We injected 1pl of 100 ng/μl vector into the cytoplasm of fertilized eggs. All injections were performed using a manipulator (MM-89, Narishige, Tokyo, Japan) with a piezo-electric actuator (PMM Controller, model PMAS-CT150; Prime Tech, Tsukuba, Japan) in HEPES-buffered CZB medium (99) under an inverted microscope (IX-71; Olympus, Nagano, Japan). After injection, embryos were cultured in 50 μl droplets of CZB supplemented with 5.56 mM D-glucose at 37°C with a humidified atmosphere of 5% CO_2 in air (100). The developmental stage of each embryo was observed and scored until 4 days in culture.

SUPPLEMENTARY MATERIAL

Supplementary Material is available at HMG Online.

ACKNOWLEDGEMENTS

We would like to thank Drs Chris Ottolenghi and David Schlessinger for discussion, Mr Yong Qian for helping the data analysis and Drs Kazuhiro Aiba, Ryo Matoba and Wendy Kimber for technical advices. T.H. and M.G.C. acknowledge post-doctoral fellowships from The Serono Foundation and The NIGMS PRAT program, respectively.

REFERENCES

1. Klein, J. and Sauer, M.V. (2001) Assessing fertility in women of advanced reproductive age. *Am. J. Obstet. Gynecol.*, **185**, 758–770.
2. Armstrong, D.T. (2001) Effects of maternal age on oocyte developmental competence. *Theriogenology*, **55**, 1303–1322.

3. ASRM/SART (2000) Assisted reproductive technology in the United States: 1997 results generated from the American Society for Reproductive Medicine/Society for Assisted Reproductive Technology Registry. *Fertil. Steril.*, **74**, 641–653 (discussion 653–654).
4. van Kooij, R.J., Looman, C.W., Habbema, J.D., Dorland, M. and te Velde, E.R. (1996) Age-dependent decrease in embryo implantation rate after *in vitro* fertilization. *Fertil. Steril.*, **66**, 769–775.
5. Navot, D., Bergh, P.A., Williams, M.A., Garrisi, G.J., Guzman, I., Sandler, B. and Grunfeld, L. (1991) Poor oocyte quality rather than implantation failure as a cause of age-related decline in female fertility. *Lancet*, **337**, 1375–1377.
6. Eichenlaub-Ritter, U. (1996) Parental age-related aneuploidy in human germ cells and offspring: a story of past and present. *Environ. Mol. Mutagen.*, **28**, 211–236.
7. Templeton, A. (2002) Ooplasmic transfer—proceed with care. *N. Engl. J. Med.*, **346**, 773–775.
8. Takeuchi, T., Ergun, B., Huang, T.H., Rosenwaks, Z. and Palermo, G.D. (1999) A reliable technique of nuclear transplantation for immature mammalian oocytes. *Hum. Reprod.*, **14**, 1312–1317.
9. Cohen, J., Scott, R., Alikani, M., Schimmel, T., Munne, S., Levron, J., Wu, L., Brenner, C., Warner, C. and Willadsen, S. (1998) Ooplasmic transfer in mature human oocytes. *Mol. Hum. Reprod.*, **4**, 269–280.
10. Levron, J., Willadsen, S., Bertoli, M. and Cohen, J. (1996) The development of mouse zygotes after fusion with synchronous and asynchronous cytoplasm. *Hum. Reprod.*, **11**, 1287–1292.
11. Meirelles, F.V. and Smith, L.C. (1997) Mitochondrial genotype segregation in a mouse heteroplasmic lineage produced by embryonic karyoplast transplantation. *Genetics*, **145**, 445–451.
12. Malter, H.E. and Cohen, J. (2002) Ooplasmic transfer: animal models assist human studies. *Reprod. Biomed. Online*, **5**, 26–35.
13. Hawes, S.M., Sapienza, C. and Latham, K.E. (2002) Ooplasmic donation in humans: the potential for epigenic modifications. *Hum. Reprod.*, **17**, 850–852.
14. Latham, K.E. (1999) Epigenetic modification and imprinting of the mammalian genome during development. *Curr. Top. Dev. Biol.*, **43**, 1–49.
15. Zhang, J., Zhuang, G.G., Zeng, Y., Acosta, C., Shu, Y. and Grifo, J. (2003) Pregnancy derived from human nuclear transfer. *Fertil. Steril.*, **80** (Suppl. 3), S56.
16. Barritt, J.A., Brenner, C.A., Malter, H.E. and Cohen, J. (2001) Mitochondria in human offspring derived from ooplasmic transplantation. *Hum. Reprod.*, **16**, 513–516.
17. Brenner, C.A., Barritt, J.A., Willadsen, S. and Cohen, J. (2000) Mitochondrial DNA heteroplasmy after human ooplasmic transplantation. *Fertil. Steril.*, **74**, 573–578.
18. Schlessinger, D. and Van Zant, G. (2001) Does functional depletion of stem cells drive aging? *Mech. Ageing Dev.*, **122**, 1537–1553.
19. Kirkwood, T.B. (1998) Ovarian ageing and the general biology of senescence. *Maturitas*, **30**, 105–111.
20. Dorland, M., van Kooij, R.J. and te Velde, E.R. (1998) General ageing and ovarian ageing. *Maturitas*, **30**, 113–118.
21. Van Zant, G. and Liang, Y. (2003) The role of stem cells in aging. *Exp. Hematol.*, **31**, 659–672.
22. Finkel, T. and Holbrook, N.J. (2000) Oxidants, oxidative stress and the biology of ageing. *Nature*, **408**, 239–247.
23. Johnson, F.B., Sinclair, D.A. and Guarente, L. (1999) Molecular biology of aging. *Cell*, **96**, 291–302.
24. Lee, C.K., Allison, D.B., Brand, J., Weindruch, R. and Prolla, T.A. (2002) Transcriptional profiles associated with aging and middle age-onset caloric restriction in mouse hearts. *Proc. Natl Acad. Sci. USA*, **99**, 14988–14993.
25. Lee, C.K., Klopp, R.G., Weindruch, R. and Prolla, T.A. (1999) Gene expression profile of aging and its retardation by caloric restriction. *Science*, **285**, 1390–1393.
26. Ly, D.H., Lockhart, D.J., Lerner, R.A. and Schultz, P.G. (2000) Mitotic misregulation and human aging. *Science*, **287**, 2486–2492.
27. Johnson, J., Canning, J., Kaneko, T., Pru, J.K. and Tilly, J.L. (2004) Germline stem cells and follicular renewal in the postnatal mammalian ovary. *Nature*, **428**, 145–150.
28. Bachvarova, R. (1985) Gene expression during oogenesis and oocyte development in mammals. *Dev. Biol. (NY)*, **1**, 453–524.
29. Jenuth, J.P., Peterson, A.C., Fu, K. and Shoubridge, E.A. (1996) Random genetic drift in the female germline explains the rapid segregation of mammalian mitochondrial DNA. *Nat. Genet.*, **14**, 146–151.
30. Carter, M.G., Hamatani, T., Sharov, A.A., Carmack, C.E., Qian, Y., Aiba, K., Ko, N.T., Dudekula, D.B., Brzoska, P.M., Hwang, S.S. *et al.* (2003) *In situ*-synthesized novel microarray optimized for mouse stem cell and early developmental expression profiling. *Genome Res.*, **13**, 1011–1021.
31. Sharov, A.A., Piao, Y., Matoba, R., Dudekula, D.B., Qian, Y., VanBuren, V., Falco, G., Martin, P.R., Stagg, C.A., Bassey, U.C. *et al.* (2003) Transcriptome analysis of mouse stem cells and early embryos. *PloS. Biol.*, **1**, E74.
32. Hamatani, T., Carter, M.G., Sharov, A.A. and Ko, M.S. (2004) Dynamics of global gene expression changes during mouse preimplantation development. *Dev. Cell*, **6**, 117–131.
33. Gene Ontology Consortium (2001) Creating the gene ontology resource: design and implementation. *Genome Res.*, **11**, 1425–1433.
34. Dahlquist, K.D., Salomonis, N., Vranizan, K., Lawlor, S.C. and Conklin, B.R. (2002) GenMAPP, a new tool for viewing and analyzing microarray data on biological pathways. *Nat. Genet.*, **31**, 19–20.
35. Doniger, S.W., Salomonis, N., Dahlquist, K.D., Vranizan, K., Lawlor, S.C. and Conklin, B.R. (2003) MAPPFinder: using gene ontology and GenMAPP to create a global gene-expression profile from microarray data. *Genome Biol.*, **4**, R7.
36. Van Blerkom, J., Sinclair, J. and Davis, P. (1998) Mitochondrial transfer between oocytes: potential applications of mitochondrial donation and the issue of heteroplasmy. *Hum. Reprod.*, **13**, 2857–2868.
37. El Mouatassim, S., Guerin, P. and Menezo, Y. (1999) Expression of genes encoding antioxidant enzymes in human and mouse oocytes during the final stages of maturation. *Mol. Hum. Reprod.*, **5**, 720–725.
38. Noda, Y., Matsumoto, H., Umaoka, Y., Tatsumi, K., Kishi, J. and Mori, T. (1991) Involvement of superoxide radicals in the mouse two-cell block. *Mol. Reprod. Dev.*, **28**, 356–360.
39. Matsui, M., Oshima, M., Oshima, H., Takaku, K., Maruyama, T., Yodoi, J. and Taketo, M.M. (1996) Early embryonic lethality caused by targeted disruption of the mouse thioredoxin gene. *Dev. Biol.*, **178**, 179–185.
40. Cuervo, A.M. and Dice, J.F. (1998) How do intracellular proteolytic systems change with age? *Front. Biosci.*, **3**, D25–D43.
41. Verbeke, P., Fonager, J., Clark, B.F. and Rattan, S.I. (2001) Heat shock response and ageing: mechanisms and applications. *Cell Biol. Int.*, **25**, 845–857.
42. Sitte, N., Huber, M., Grune, T., Ladhoff, A., Doecke, W.D., Von Zglinicki, T. and Davies, K.J. (2000) Proteasome inhibition by lipofuscin/ceroid during postmitotic aging of fibroblasts. *FASEB J.*, **14**, 1490–1498.
43. Cogswell, P.C., Kashatus, D.F., Keifer, J.A., Guttridge, D.C., Reuther, J.Y., Bristow, C., Roy, S., Nicholson, D.W. and Baldwin, A.S., Jr (2003) NF-kappa B and I kappa B alpha are found in the mitochondria. Evidence for regulation of mitochondrial gene expression by NF-kappa B. *J. Biol. Chem.*, **278**, 2963–2968.
44. Bershadsky, A.D., Gelfand, V.I., Svitkina, T.M. and Tint, I.S. (1980) Destruction of microfilament bundles in mouse embryo fibroblasts treated with inhibitors of energy metabolism. *Exp. Cell Res.*, **127**, 421–429.
45. Tarin, J.J. (1996) Potential effects of age-associated oxidative stress on mammalian oocytes/embryos. *Mol. Hum. Reprod.*, **2**, 717–724.
46. Tarin, J.J., Perez-Albala, S. and Cano, A. (2000) Consequences on offspring of abnormal function in ageing gametes. *Hum. Reprod. Update*, **6**, 532–549.
47. Edelmann, W., Umar, A., Yang, K., Heyer, J., Kucherlapati, M., Lia, M., Kneitz, B., Avdievich, E., Fan, K., Wong, E. *et al.* (2000) The DNA mismatch repair genes *Msh3* and *Msh6* cooperate in intestinal tumor suppression. *Cancer Res.*, **60**, 803–807.
48. Wei, K., Clark, A.B., Wong, E., Kane, M.F., Mazur, D.J., Parris, T., Kolas, N.K., Russell, R., Hou, H., Jr, Kneitz, B. *et al.* (2003) Inactivation of Exonuclease 1 in mice results in DNA mismatch repair defects, increased cancer susceptibility and male and female sterility. *Genes Dev.*, **17**, 603–614.
49. Prolla, T.A., Baker, S.M., Harris, A.C., Tsao, J.L., Yao, X., Bronner, C.E., Zheng, B., Gordon, M., Reneker, J., Arnheim, N. *et al.* (1998) Tumour susceptibility and spontaneous mutation in mice deficient in Mlh1, Pms1 and Pms2 DNA mismatch repair. *Nat. Genet.*, **18**, 276–279.
50. Chang, C.L., Marra, G., Chauhan, D.P., Ha, H.T., Chang, D.K., Ricciardiello, L., Randolph, A., Carethers, J.M. and Boland, C.R. (2002) Oxidative stress inactivates the human DNA mismatch repair system. *Am. J. Physiol. Cell Physiol.*, **283**, C148–C154.

51. Keefe, D., Franco, S., Liu, L., Trimarchi, J., Blasco, M. and Weitzen, S. (2003) Short telomeres in the chromosomes of spare eggs predict poor prognosis following *in vitro* fertilization/embryo transfer—toward a telomere theory of reproductive aging in women. *Fertil. Steril.*, **80** (Suppl. 3), S1.
52. Vitt, U.A., Mazerbourg, S., Klein, C. and Hsueh, A.J. (2002) Bone morphogenetic protein receptor type II is a receptor for growth differentiation factor-9. *Biol. Reprod.*, **67**, 473–480.
53. Erickson, G.F. and Shimasaki, S. (2003) The spatiotemporal expression pattern of the bone morphogenetic protein family in rat ovary cell types during the estrous cycle. *Reprod. Biol. Endocrinol.*, **1**, 9.
54. Hayashi, K., Kobayashi, T., Umino, T., Goitsuka, R., Matsui, Y. and Kitamura, D. (2002) SMAD1 signaling is critical for initial commitment of germ cell lineage from mouse epiblast. *Mech. Dev.*, **118**, 99–109.
55. Fritz, B.R. and Sheets, M.D. (2001) Regulation of the mRNAs encoding proteins of the BMP signaling pathway during the maternal stages of *Xenopus* development. *Dev. Biol.*, **236**, 230–243.
56. Lippincott-Schwartz, J., Yuan, L.C., Bonifacino, J.S. and Klausner, R.D. (1989) Rapid redistribution of Golgi proteins into the ER in cells treated with brefeldin A: evidence for membrane cycling from Golgi to ER. *Cell*, **56**, 801–813.
57. Moreno, R.D., Schatten, G. and Ramalho-Santos, J. (2002) Golgi apparatus dynamics during mouse oocyte *in vitro* maturation: effect of the membrane trafficking inhibitor brefeldin A. *Biol. Reprod.*, **66**, 1259–1266.
58. Iwahashi, K., Kuji, N., Fujiwara, T., Tanaka, H., Takahashi, J., Inagaki, N., Komatsu, S., Yamamoto, A., Yoshimura, Y. and Akagawa, K. (2003) Expression of the exocytotic protein syntaxin in mouse oocytes. *Reproduction*, **126**, 73–81.
59. Rankin, T., Talbot, P., Lee, E. and Dean, J. (1999) Abnormal zonae pellucidae in mice lacking ZP1 result in early embryonic loss. *Development*, **126**, 3847–3855.
60. Rankin, T.L., O'Brien, M., Lee, E., Wigglesworth, K., Eppig, J. and Dean, J. (2001) Defective zonae pellucidae in Zp2-null mice disrupt folliculogenesis, fertility and development. *Development*, **128**, 1119–1126.
61. Liu, C., Litscher, E.S., Mortillo, S., Sakai, Y., Kinloch, R.A., Stewart, C.L. and Wassarman, P.M. (1996) Targeted disruption of the *mZP3* gene results in production of eggs lacking a zona pellucida and infertility in female mice. *Proc. Natl Acad. Sci. USA*, **93**, 5431–5436.
62. Rankin, T., Familari, M., Lee, E., Ginsberg, A., Dwyer, N., Blanchette-Mackie, J., Drago, J., Westphal, H. and Dean, J. (1996) Mice homozygous for an insertional mutation in the *Zp3* gene lack a zona pellucida and are infertile. *Development*, **122**, 2903–2910.
63. Webster, K.A., Prentice, H. and Bishopric, N.H. (2001) Oxidation of zinc finger transcription factors: physiological consequences. *Antioxid. Redox Signal.*, **3**, 535–548.
64. Allen, R.G. and Tresini, M. (2000) Oxidative stress and gene regulation. *Free Radic. Biol. Med.*, **28**, 463–499.
65. Park, I.K., Morrison, S.J. and Clarke, M.F. (2004) Bmi1, stem cells and senescence regulation. *J. Clin. Invest.*, **113**, 175–179.
66. O'Carroll, D., Erhardt, S., Pagani, M., Barton, S.C., Surani, M.A. and Jenuwein, T. (2001) The polycomb-group gene *Ezh2* is required for early mouse development. *Mol. Cell. Biol.*, **21**, 4330–4336.
67. Lopatina, N., Haskell, J.F., Andrews, L.G., Poole, J.C., Saldanha, S. and Tollefsbol, T. (2002) Differential maintenance and *de novo* methylating activity by three DNA methyltransferases in aging and immortalized fibroblasts. *J. Cell. Biochem.*, **84**, 324–334.
68. Bertram, M.J., Berube, N.G., Hang-Swanson, X., Ran, Q., Leung, J.K., Bryce, S., Spurgers, K., Bick, R.J., Baldini, A., Ning, Y. *et al.* (1999) Identification of a gene that reverses the immortal phenotype of a subset of cells and is a member of a novel family of transcription factor-like genes. *Mol. Cell. Biol.*, **19**, 1479–1485.
69. Tong, Z.B., Gold, L., Pfeifer, K.E., Dorward, H., Lee, E., Bondy, C.A., Dean, J. and Nelson, L.M. (2000) Mater, a maternal effect gene required for early embryonic development in mice. *Nat. Genet.*, **26**, 267–268.
70. Tong, Z.B., Bondy, C.A., Zhou, J. and Nelson, L.M. (2002) A human homologue of mouse Mater, a maternal effect gene essential for early embryonic development. *Hum. Reprod.*, **17**, 903–911.
71. Tschopp, J., Martinon, F. and Burns, K. (2003) NALPs: a novel protein family involved in inflammation. *Nat. Rev. Mol. Cell. Biol.*, **4**, 95–104.
72. Bateman, A., Birney, E., Cerruti, L., Durbin, R., Etwiller, L., Eddy, S.R., Griffiths-Jones, S., Howe, K.L., Marshall, M. and Sonnhammer, E.L. (2002) The Pfam protein families database. *Nucl. Acids Res.*, **30**, 276–280.
73. Altschul, S.F. and Gish, W. (1996) Local alignment statistics. *Methods Enzymol.*, **266**, 460–480.
74. Davuluri, R.V., Grosse, I. and Zhang, M.Q. (2001) Computational identification of promoters and first exons in the human genome. *Nat. Genet.*, **29**, 412–417.
75. Saitou, N. and Nei, M. (1987) The neighbor-joining method: a new method for reconstructing phylogenetic trees. *Mol. Biol. Evol.*, **4**, 406–425.
76. Schwartz, S., Zhang, Z., Frazer, K.A., Smit, A., Riemer, C., Bouck, J., Gibbs, R., Hardison, R. and Miller, W. (2000) PipMaker—a web server for aligning two genomic DNA sequences. *Genome Res.*, **10**, 577–586.
77. Svoboda, P., Stein, P., Hayashi, H. and Schultz, R.M. (2000) Selective reduction of dormant maternal mRNAs in mouse oocytes by RNA interference. *Development*, **127**, 4147–4156.
78. Kim, M.H., Yuan, X., Okumura, S. and Ishikawa, F. (2002) Successful inactivation of endogenous *Oct-3/4* and *c-mos* genes in mouse preimplantation embryos and oocytes using short interfering RNAs. *Biochem. Biophys. Res. Commun.*, **296**, 1372–1377.
79. Wianny, F. and Zernicka-Goetz, M. (2000) Specific interference with gene function by double-stranded RNA in early mouse development. *Nat. Cell. Biol.*, **2**, 70–75.
80. Stein, P., Svoboda, P. and Schultz, R.M. (2003) Transgenic RNAi in mouse oocytes: a simple and fast approach to study gene function. *Dev. Biol.*, **256**, 187–193.
81. Haraguchi, S., Saga, Y., Naito, K., Inoue, H. and Seto, A. (2004) Specific gene silencing in the pre-implantation stage mouse embryo by an siRNA expression vector system. *Mol. Reprod. Dev.*, **68**, 17–24.
82. Kitagawa, T., Suganuma, N., Nawa, A., Kikkawa, F., Tanaka, M., Ozawa, T. and Tomoda, Y. (1993) Rapid accumulation of deleted mitochondrial deoxyribonucleic acid in postmenopausal ovaries. *Biol. Reprod.*, **49**, 730–736.
83. Keefe, D.L., Niven-Fairchild, T., Powell, S. and Buradagunta, S. (1995) Mitochondrial deoxyribonucleic acid deletions in oocytes and reproductive aging in women. *Fertil. Steril.*, **64**, 577–583.
84. Tarin, J.J., Perez-Albala, S. and Cano, A. (2001) Cellular and morphological traits of oocytes retrieved from aging mice after exogenous ovarian stimulation. *Biol. Reprod.*, **65**, 141–150.
85. Tarin, J.J., Vendrell, F.J., Ten, J. and Cano, A. (1998) Antioxidant therapy counteracts the disturbing effects of diamide and maternal ageing on meiotic division and chromosomal segregation in mouse oocytes. *Mol. Hum. Reprod.*, **4**, 281–288.
86. Schon, E.A., Kim, S.H., Ferreira, J.C., Magalhaes, P., Grace, M., Warburton, D. and Gross, S.J. (2000) Chromosomal non-disjunction in human oocytes: is there a mitochondrial connection? *Hum. Reprod.*, **15** (Suppl. 2), 160–172.
87. Wakayama, T., Perry, A.C., Zuccotti, M., Johnson, K.R. and Yanagimachi, R. (1998) Full-term development of mice from enucleated oocytes injected with cumulus cell nuclei. *Nature*, **394**, 369–374.
88. Humpherys, D., Eggan, K., Akutsu, H., Hochedlinger, K., Rideout, W.M., III, Biniszkiewicz, D., Yanagimachi, R. and Jaenisch, R. (2001) Epigenetic instability in ES cells and cloned mice. *Science*, **293**, 95–97.
89. Wilmut, I., Beaujean, N., De Sousa, P.A., Dinnyes, A., King, T.J., Paterson, L.A., Wells, D.N. and Young, L.E. (2002) Somatic cell nuclear transfer. *Nature*, **419**, 583–587.
90. McCarroll, S.A., Murphy, C.T., Zou, S., Pletcher, S.D., Chin, C.S., Jan, Y.N., Kenyon, C., Bargmann, C.I. and Li, H. (2004) Comparing genomic expression patterns across species identifies shared transcriptional profile in aging. *Nat. Genet.*, **36**, 197–204.
91. Tatar, M., Bartke, A. and Antebi, A. (2003) The endocrine regulation of aging by insulin-like signals. *Science*, **299**, 1346–1351.
92. Downs, S.M., Humpherson, P.G. and Leese, H.J. (2002) Pyruvate utilization by mouse oocytes is influenced by meiotic status and the cumulus oophorus. *Mol. Reprod. Dev.*, **62**, 113–123.
93. Biggers, J.D., Whittingham, D.G. and Donahue, R.P. (1967) The pattern of energy metabolism in the mouse oocyte and zygote. *Proc. Natl Acad. Sci. USA*, **58**, 560–567.
94. Ramalho-Santos, M., Yoon, S., Matsuzaki, Y., Mulligan, R.C. and Melton, D.A. (2002) 'Stemness': transcriptional profiling of embryonic and adult stem cells. *Science*, **298**, 597–600.

95. Benjamini, Y. and Hochberg, Y. (1995) Controlling the false discovery rate—a practical and powerful approach to multiple testing. *J. R. Stat. Soc. B*, **67**, 289–300.
96. Schena, M., Shalon, D., Davis, R.W. and Brown, P.O. (1995) Quantitative monitoring of gene expression patterns with a complementary DNA microarray. *Science*, **270**, 467–470.
97. Baldi, P. and Long, A.D. (2001) A Bayesian framework for the analysis of microarray expression data: regularized *t*-test and statistical inferences of gene changes. *Bioinformatics*, **17**, 509–519.
98. Hogan, B.L.M., Beddington, R., Costantini, F. and Elizabeth, L. (1994) *Manipulating the Mouse Embryo: A Laboratory Manual*, 2nd edn. Cold Spring Harbor Laboratory.
99. Kimura, Y. and Yanagimachi, R. (1995) Intracytoplasmic sperm injection in the mouse. *Biol. Reprod.*, **52**, 709–720.
100. Akutsu, H., Tres, L.L., Tateno, H., Yanagimachi, R. and Kierszenbaum, A.L. (2001) Offspring from normal mouse oocytes injected with sperm heads from the azh/azh mouse display more severe sperm tail abnormalities than the original mutant. *Biol. Reprod.*, **64**, 249–256.